RAPID COMMUNICATIONS IN MASS SPECTROMETRY
Rapid Commun. Mass Spectrom. 2007; **21**: 3395–3408
Published online in Wiley InterScience (www.interscience.wiley.com) DOI: 10.1002/rcm.3213

Tandem mass spectrometry acquisition approaches to enhance identification of protein-protein interactions using low-energy collision-induced dissociative chemical crosslinking reagents

Erik J. Soderblom, Benjamin G. Bobay, John Cavanagh and Michael B. Goshe*
Department of Molecular and Structural Biochemistry, North Carolina State University, Raleigh, NC 27695-7622, USA

Received 7 May 2007; Revised 25 July 2007; Accepted 12 August 2007

Chemical crosslinking combined with mass spectrometry is a useful tool for studying the topological organization of multiprotein interactions, but it is technically challenging to identify peptides involved in a crosslink using tandem mass spectrometry (MS/MS) due to the presence of product ions originating from both peptides within the same crosslink. We have previously developed a novel set of collision-induced dissociative chemical crosslinking reagents (CID-CXL reagents) that incorporate a labile bond within the linker which readily dissociates at a single site under low-energy collision-induced dissociation (CID) to enable independent isolation and sequencing of the crosslinked peptides by traditional MS/MS and database searching. Alternative low-energy CID events were developed within the in-source region by increasing the multipole DC offset voltage (ISCID) or within the ion trap by increasing the collisional excitation (ITCID). Both dissociation events, each having their unique advantages, occur without significant backbone fragmentation to the peptides, thus permitting subsequent CID to be applied to these distinct peptide ions for generation of suitable product ion spectra for database searching. Each approach was developed and applied to a chemical crosslinking study involving the N-terminal DNA-binding domain of AbrB (AbrBN), a transition-state regulator in *Bacillus subtilis*. A total of thirteen unique crosslinks were identified using the ITCID approach which represented a significant improvement over the eight unique crosslinks identified using the ISCID approach. The ability to segregate intrapeptide and interpeptide crosslinks using ITCID represents the first step towards high-throughput analysis of protein-protein crosslinks using our CID-CXL reagents. Copyright © 2007 John Wiley & Sons, Ltd.

Chemical crosslinking combined with mass spectrometry (MS) has become a viable approach to study the low-resolution structures of protein and protein complexes.[1] These experiments often employ the use of bifunctional crosslinking reagents to covalently attach the side chains of two residues within a defined spatial proximity. A set of maximal distance constraints is then generated based on the residues involved in the crosslink. In addition to identifying unknown components within a multiprotein ensemble, these constraints can offer insight into the spatial orientations of a protein complex when used in conjunction with molecular modeling.[2–4] Crosslinking can also complement high-resolution techniques such as multidimensional nuclear magnetic resonance (NMR) or X-ray crystallography to study the structures of protein complexes because measurements can be performed under a wide range of conditions that mimic native protein environments and permit examination of protein complex formation not suitable with high-resolution techniques.

Despite the straightforwardness of these experiments, the unambiguous identification of crosslinked species remains technically challenging using liquid chromatography/tandem mass spectrometry (LC/MS/MS) for several reasons. A major factor is the complexity of the sample resulting from the proteolytic digestion of the crosslinked proteins.[5] These mixtures contain many non-derivatized peptides which could preclude detection of the low abundant crosslinked species of interest due to co-elution and electrospray ionization (ESI) suppression effects. There are also derivatized dead-end products formed during the crosslinking reaction. Although these modifications provide information on surface accessibility of the particular residues involved, they offer no structural information regarding distance constraints, and, in essence, contribute to sample complexity.

Another difficulty is the recognition of the peptide-peptide crosslinks as detected by the mass spectrometer. Typically,

**Correspondence to*: M. B. Goshe, Department of Molecular and Structural Biochemistry, North Carolina State University, 128 Polk Hall, Campus Box 7622, Raleigh, NC 27695-7622, USA.
E-mail: michael_goshe@ncsu.edu
Contract/grant sponsor: North Carolina State University and the North Carolina Agricultural Research Service.

these low abundant crosslinked species require the use of high mass measurement accuracy analyzers with requisite high resolution and sensitivity to identify potential crosslinked peptides. Spectra resulting from collision-induced dissociation (CID) contain product ions originating from both peptides involved in the crosslink and thus complicate spectral interpretation. Since current versions of database-searching algorithms such as SEQUEST and Mascot cannot match crosslinked product ion spectra, data analysis often requires the use of multiple third party software solutions. Programs such as Automated Spectrum Assignment Program (ASAP),[4] MS2Assign,[6] and SearchXLinks[7] are freely available web-based applications. However, these tools require a significant input from the user and manual validation of the spectra to recognize crosslinked products. Even with more advanced MS instrumentation and software to analyze the products, identification of the crosslinked species only works moderately well and is still highly dependent on protein size and complexity.

To make better use of MS analysis for elucidation of protein crosslinks, several advances in crosslinker design have been implemented over the last few years. They include the use of isotopically coded reagents,[8,9] enrichment of crosslinked products through affinity tags,[10,11] and MS-cleavable crosslinking reagents.[12,13] Examples of MS-cleavable reagents include a reagent which yields a stable benzyl cation marker ion upon CID.[12] Although this reagent provides a marker for locating potentially crosslinked peptides, subsequent MS/MS verification is still difficult because the peptide-peptide crosslink remains intact. Recently, Tang *et al*. described a reagent which, upon low-energy CID, specifically dissociates the reagent at two locations within the linker region.[13] This results in a marker ion and two individual peptides which can be analyzed separately. However, the design of the reagent incorporates a spacer arm length of 43.0 Å which is much longer than the preferred length of 8.0 to 15.0 Å which is the most useful distance geometry information for threading calculations.[14,15] In our approach we have developed novel crosslinking reagents within the preferred length range that incorporate a novel aspartyl-prolyl bond within the linker which readily dissociates at a single site under low-energy CID conditions.[16] This design allows for independent isolation and sequencing of the crosslinked peptides by traditional MS/MS and database-searching techniques. Our goal is to use this concept of single-site gas-phase cleavable chemical crosslinkers to develop high-throughput approaches to identify protein-protein and protein-nucleic acid interactions that can be universally applied to all LC/MS/MS platforms.

In our initial report, the dissociation of crosslinked complexes occurred within the in-source region of the mass spectrometer (in-source CID, ISCID), followed by subsequent MS/MS (MS^2) analysis of the four most abundant ions.[16] Although this ISCID-MS^2 acquisition approach worked reasonably well, ISCID-based dissociation of the crosslinked complexes did not always result in the individual peptides being among the four most abundant ions. Since our strategy is predicated on data-dependent acquisition to capture and subsequently fragment each individual peptide involved in a crosslink, non-efficient dissociation of the crosslinked complexes will limit the number of crosslink identifications. To improve our method, we utilized the general mechanism of our reagent's selective dissociation to achieve effective dissociation of crosslinked complexes within the ion trap (in-trap CID, ITCID) of the mass spectrometer using an MS^2 event with subsequent fragmentation of the individual peptides with an MS^3 event. This ITCID-MS^3 acquisition approach was developed using one of our CID-CXL-MS/MS reagents to crosslink the N-terminal DNA-binding domain of antibiotic resistance protein B (AbrBN – residues 1–53), a well-studied transition-state regulator in *Bacillus subtilis*. The identification of intrapeptide, interpeptide, and dead-end crosslink products of AbrBN using both ISCID-MS^2 and ITCID-MS^3 approaches is discussed. Since the NMR structure of the N-terminal homodimer is available,[17,18] this model also permitted the evaluation of each acquisition approach based on the identification of protein crosslinks using database-searching techniques.

EXPERIMENTAL

Materials

Fmoc-protected amino acids and NovaSyn TGT resin were from EMD Biosciences (San Diego, CA, USA). AbrBN was overexpressed and purified as previously described.[19] Sequencing-grade modified trypsin was purchased from Promega (Madison, WI, USA). Acetonitrile (HPLC grade) and formic acid (ACS reagent grade) were from Aldrich (Milwaukee, WI, USA). Water was distilled and purified using a High-Q 103S water purification system (Wilmette, IL, USA). All other chemicals were from Sigma/Aldrich/Fluka (http://www.sigmaaldrich.com) unless otherwise stated.

Synthesis of bisuccinimidyl-succinamyl-aspartyl-proline (SuDP)

SuDP linker region synthesis and esterification using N-hydroxysuccinimide were performed as previously described.[16] Before use, the aspartyl side chain *tert*-butyl-protecting group was deprotected by addition of 95% trifluoroacetic acid (TFA)/5% water with gentle stirring at room temperature for 30 min. The deprotected sample was then purified by high-performance liquid chromatography (HPLC) to isolate the doubly esterified product from singly esterified or non-esterified product which could have resulted from acid-mediated hydrolysis during deprotection of the aspartyl side chain. Fractions corresponding to the doubly esterified deprotected reagent were collected, dried under vacuum, and subsequently stored at −80°C until use.

Crosslinking and proteolytic digestion of AbrBN

A stock solution of 530 μM AbrBN in 50 mM Na_2HPO_4, 10 mM NaCl, 1 mM dithiothreitol (DTT), 1 mM EDTA, pH 7.8, was dialyzed into 25 mM Na_2HPO_4, 1 mM DTT, 1 mM EDTA, pH 7.8, overnight and then diluted with dialysis buffer to produce 50 μM AbrBN. Aliquots of SuDP crosslinking reagent resuspended in dimethyl sulfoxide (DMSO) were added to 30 μL of the protein solution to produce final protein-to-crosslinker ratios of 1:2, 1:5, 1:10, 1:20, 1:30, and 1:40. The final organic solvent concentration was kept below 3% of the total volume for each reaction.

DOI: 10.1002/rcm

Crosslinking was performed at ambient temperature with gentle stirring for 30 min followed by quenching with 1 M Tris, pH 9.0, to produce a final concentration of 10 mM, and the solution was incubated for 15 min at ambient temperature. To determine an effective protein-to-crosslinker ratio, samples containing various ratios were prepared and analyzed by sodium dodecyl sulfate polyacrylamide gel electrophoresis (SDS- PAGE) using an 18% SDS-Tris/Tricine-PAGE gel with visualization of the protein bands by Coomassie staining. Based on this SDS-PAGE analysis, AbrBN samples crosslinked using 1:2 and 1:5 protein-to-crosslinker ratios were diluted to 500 μL with 50 mM NH_4HCO_3, pH 8.0, and digested with either trypsin (1:50, w/w) or chymotrypsin (1:50, w/w) overnight at 37°C or for 5 h at ambient temperature, respectively. Samples were purified by solid-phase extraction using a Prevail C_{18} Extract-Clean column (Alltech Technologies Inc., Deerfield, IL, USA) connected to a vacuum manifold, dried via vacuum centrifugation, and stored at −80°C until use.

LC/MS/MS analysis

Crosslinked peptide samples were separated using an Agilent 1100 Series capillary LC system (Agilent Technologies, Inc., Palo Alto, CA, USA) coupled directly on-line with an LCQ Deca ion trap mass spectrometer (Thermo Finnigan, San Jose, CA, USA). The mass spectrometer was equipped with an in-house manufactured electrospray ionization (ESI) interface using an electrospray voltage of 2.2 kV in the positive ion mode. Reversed-phase HPLC separation of peptides was accomplished using a 150 μm i.d. × 40 cm length fused-silica capillary (Polymicro Technologies Inc., Phoenix, AZ, USA) slurry-packed with 5 μm Jupiter C_{18} stationary phase (Phenomenex, Torrance, CA, USA). The mobile phases consisted of (A) 0.1% formic acid in water and (B) 0.1% formic acid in acetonitrile. After loading approximately 4 μg of total peptide digest onto the reversed-phase column, the mobile phase was held at 5% B for 20 min and the peptides were eluted using a linear gradient of 0.5% B/min to 95% B at a flow rate of 1.5 μL/min.

Data-dependent acquisition using ISCID-MS^2 and ITCID-MS^3

For an ISCID-MS^2 acquisition, a series of six continuously repeating scan events were employed. The first scan event was a 'survey' MS scan from *m/z* 400 to 2000 followed by a CID-CXL dissociation scan from *m/z* 400 to 2000 which implemented an additional potential offset of 15 V to the multipole region of the instrument. In a data-dependent process, the four most intense ions from the CID-CXL dissociation scan were sequentially captured and subjected to MS/MS analysis using a normalized collision energy setting of 45% in scan events three through six. To increase the selective capture of lower abundant precursor ions, a 2 min dynamic exclusion list was implemented.

For an ITCID-MS^3 acquisition, a series of four continuously repeating scan events were employed. The first scan event was a survey MS scan from *m/z* 400 to 2000. In the second scan event (the CID-CXL dissociation scan for precursor crosslinked species), the most intense ion from the survey MS scan was data-dependently selected and subjected to MS/MS analysis using a normalized collision energy setting of 45%. The two most intense ions from the second scan were then data-dependently selected and individually subjected to an MS^3 analysis with a normalized collision energy setting of 45% during scan events three and four. To increase the selective capture of lower abundant precursor ions data were acquired using no dynamic exclusion list, a 12 s dynamic exclusion list, and a 2 min dynamic exclusion list.

Analysis of crosslinked products using ISCID-MS^2 and ITCID-MS^3

All product ion spectra resulting from ISCID-MS^2 and ITCID-MS^3 acquisition approaches were searched using TurboSEQUEST (Bioworks 3.3, Thermo Finnigan, San Jose, CA, USA) against a database containing the AbrBN sequence from *Bacillus subtilis* appended with sequences of trypsin, chymotrypsin and those contained in the bovine proteome database obtained from the NCBI website. The bovine proteome was included in the searches to provide a database of sufficient size to increase the statistical confidence of the SEQUEST scores. All product ion spectra were searched with dynamic mass modifications on the protein N-terminus and all lysyl residues of +97.0 u (proline, P) and +197.1 u (succinimidyl aspartate, SuD), in addition to a dynamic mass modification of +16.0 u on Met residues due to methionine oxidation. To recognize product ion spectra using the ISCID-MS^2 approach, charge-dependent cross-correlation (Xcorr) scores of at least 1.9, 1.5, and 3.0 for +1, +2, and +3 charge states, respectively, and delta-cross correlation (ΔC_n) scores of 0.08 and higher were required. Product ion spectra selected by this automated search were manually inspected to validate peptide identifications.

For data acquired using the ITCID-MS^3 approach, three SEQUEST searches were performed. The first analysis included all the product ions generated during the MS/MS scan events, with peptide recognition based on the Xcorr and ΔC_n values as described for the ISCID-MS^2 approach. The second analysis interrogated all MS^3 spectra with peptide recognition based on Xcorr and ΔC_n values of 1.4, 1.3, and 2.0 for +1, +2, and +3 charge states, respectively. The use of lower SEQUEST threshold values was necessary for the product ion spectra generated by MS^3 due to fewer ions available for CID based on the MS^2 event. To increase SEQUEST scores and confidence in peptide recognition, the MS^3 product ion spectra were re-searched with group scanning of all spectra within a 30 s window that corresponded to the same precursor *m/z* (within 1.5 u). Product ion spectra selected by this grouping method were manually inspected to validate peptide identifications.

To identify a pair of crosslinked peptides using both acquisition approaches, product ion spectra corresponding to peptides recognized by SEQUEST were arranged according to retention time (i.e., scan number). These sorted results were searched for a product ion spectrum that identified the presence of a peptide with a +97.0 u (P) mass modification on a lysyl residue that was adjacent (i.e, within the peak width of the eluting peptide-peptide crosslink) to another product ion spectrum for a peptide with a +197.1 u (SuD) modification on a lysyl residue. For these pairs, the prior MS spectrum (the first MS scan event) was examined for the calculated *m/z*

DOI: 10.1002/rcm

of the intact crosslinked peptide complex. The following product ion spectrum (the second MS scan event) was examined for the presence of the two individual peptide product ions generated from dissociation at the aspartyl-prolyl bond within the crosslinking reagent, which were then used to generate the subsequent tandem mass spectra used for peptide sequence identification. Additional details regarding the unique features of each approach to database searching are described in the Results and Discussion section.

RESULTS AND DISCUSSION

Crosslinking of AbrBN

To initially screen for appropriate crosslinking conditions, AbrBN was incubated with our SuDP crosslinking reagent at protein-to-crosslinker ratios as high as 1:40 and analyzed using SDS-PAGE. All crosslinking ratios above 1:5 resulted in complete dimerization of AbrBN and were therefore not chosen for further analysis, since derivatization of too many lysyl side chains may disrupt native protein structure and preclude efficient digestion using trypsin or chymotrypsin.[20,21] Protein-to-crosslinker ratios of 1:2 and 1:5 resulted in approximately 50% and 95% dimer product, respectively, and were used for all subsequent analyses (Fig. 1(A)). These ratios were considerably lower than the higher ratios of SuDP (1:100 and 1:500) used in our previous study to crosslink glutathione S-transferase.[16] This has been attributed to partial hydrolysis of the crosslinker generated during *tert*-butyl deprotection of the aspartyl side chain. To increase reagent purity, an additional HPLC purification step following deprotection has been implemented and used for all SuDP crosslinking experiments with AbrBN. Because on this additional purification, the protein-to-crosslinker ratios are in the range expected for typical crosslinking experiments.

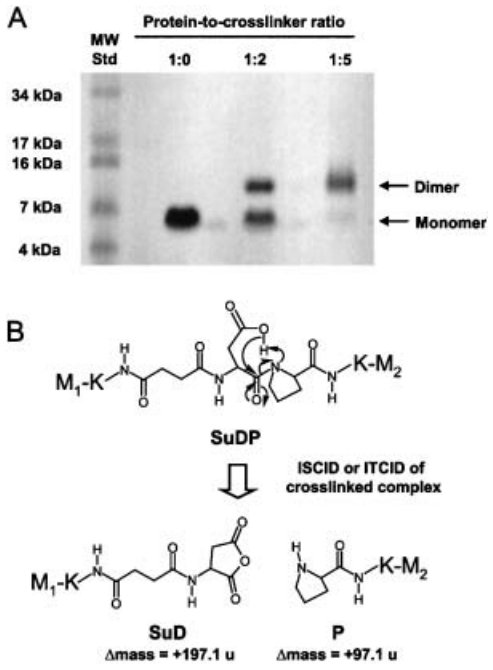

Figure 1. Crosslinking of AbrBN using CID-CXL-MS/MS reagents. (A) SDS-PAGE analysis of AbrBN crosslinked with the SuDP CID-CXL reagent at 1:0, 1:2, and 1:5 protein-to-crosslinker ratios. AbrBN monomer (6.1 kDa) and dimer (12.2 kDa) are visualized using Coomassie blue staining. (B) Proposed mechanism of the selective dissociation of the SuDP crosslink at the aspartyl-prolyl bond mediated by in-source collision-induced dissociation (ISCID) or in-trap collision-induced dissociation (ITCID). The resulting peptides, M_1 and M_2, contain an additional mass of 197.1 or 97.0 u corresponding to the residual SuD or P portion of the CID-CXL-MS/MS reagent, respectively.

Strategies for crosslinked complex dissociation and subsequent peptide analysis

Our CID-CXL reagents were designed to be integrated with automated LC/MS-based strategies which data-dependently select the most abundant precursor ions for subsequent MS/MS analysis. To be effective, crosslinked peptide complexes need to be selectively fragmented at the aspartyl-prolyl bond within the crosslinking reagent, resulting in two individual intact peptides (Fig. 1(B)) while minimizing backbone cleavage of the peptides. In our initial description of these reagents, this dissociation event was performed within the in-source region of the instrument by increasing the multipole DC offset voltage (ISCID).[16] An increased multipole offset increases the frequency with which ions collide with gases present in that region of the instrument and results in dissociation of the complex into two individual peptides. Using ISCID, we have observed that the amount of voltage required to dissociate crosslinked complexes varies and a multipole offset of 15 V does not always result in a high abundance of both intact individual peptides. This could be due to inadequate control regarding the amount and composition of the gases present within the in-source region of the instrument.

As an alternative to ISCID, we examined crosslinked complex dissociation efficiency by performing the fragmentation in the ion trap during an MS^2 event (ITCID). This approach still utilizes the selective fragmentation of an aspartyl-prolyl bond within the CID-CXL reagent, but is conducted within the ion trap where CID is more effectively controlled. By data-dependently selecting the most abundant ions from the survey MS scan and subjecting them to CID-CXL dissociation in the ion trap, the two peptides produced from the crosslinked complex can then be data-dependently selected for further fragmentation during an MS^3 event.

Crosslinks of AbrBN identified by ISCID-MS^2 and ITCID-MS^3 analysis

The results of crosslinked AbrBN analyzed using the ISCID-MS^2 approach are presented in Table 1. A total of eight unique crosslinked species were identified using this approach: two involving lysyl residues from two peptides (interpeptide crosslink) and six involving lysyl residues within the same peptide (intrapeptide crosslink). These eight unique crosslinked species corresponded to three pairs of lysyl residues. When mapped to the NMR solution structure of AbrBN (PDB: 1Z0R), the measured distances between the α-carbons of Lys2∼Lys9, Lys31∼Lys47, and Lys42∼Lys46 are 19.27 Å, 11.47 Å, and 13.02 Å, respectively, which are all within the maximum distance constraint of 23.9 Å for the SuDP reagent

DOI: 10.1002/rcm

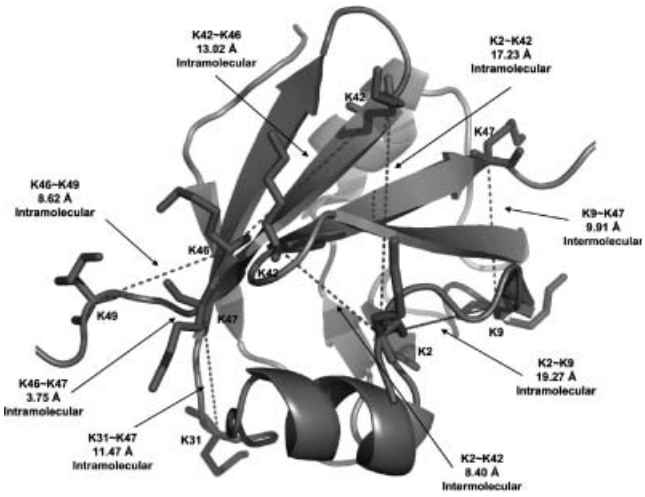

Figure 2. The NMR solution structure of the AbrBN homodimer (PDB: 1Z0R) with the identified crosslinked lysyl residues. Distance measurements from α-carbon to α-carbon of lysyl residues range between 3.75 and 19.27 Å, which are all within the maximal distance constraint of 23.9 Å for the SuDP CID-CXL-MS/MS reagent. Of the crosslinks identified, two were intermolecular (between the two subunits of AbrBN) and six were intramolecular (within the same subunit of AbrBN). It should be noted that the K2∼K42 crosslink can be either inter- or intramolecular since both versions are within the SuDP distance constraint.

(Fig. 2). Higher protein-to-crosslinker ratios had little effect on the identification of crosslinked species, as only one additional intrapeptide crosslink was identified with the sample treated with a 1:5 ratio.

The results of crosslinked AbrBN samples analyzed using the ITCID-MS^3 approach are presented in Table 2. A total of thirteen unique crosslinked species, five interpeptide and eight intrapeptide, were identified. These correspond to six unique sets of crosslinked lysyl residues, three more than using the ISCID-MS^2 approach. When mapped to the NMR solution structure of AbrBN, the measured distances between the α-carbon of all crosslinked lysyl residues are between 3.75 and 19.27 Å (Fig. 2). Unlike ISCID-MS^2, higher protein-to-crosslinker ratios had an effect on the ITCID-MS^3 identification of peptide crosslinks, as four additional crosslinked complexes were specific to either crosslinking ratio. As with ISCID-MS^2, no interpeptide crosslinks were identified with chymotrypsin due to the alternative cleavage specificity relative to trypsin that may promote larger peptide-peptide crosslinks not detectable using the ion trap data acquisition parameters. However, the intrapeptide crosslinks identified provide useful structural information regarding AbrBN that is not achievable with only trypsin digestion.

Due to the asymmetry of our CID-CXL reagent, covalent attachment to the protein can occur with two possible orientations. These two crosslink versions can be observed with AbrBN (Tables 1 and 2). These crosslinks have the same molecular mass but display different retention times during reversed-phase chromatography (data not shown). In both cases, each detected crosslinked complex can be effectively dissociated to generate two distinctly modified peptides that can be further subjected to CID analysis. Thus for a particular Lys∼Lys crosslink, each peptide is identified as containing the SuD-modification in one crosslink and the P-modification in the other. This duality may be used as a constraint to increase the confidence of crosslink identification; however, certain protein structural features may favor one orientation of the CID-CXL reagent over the other.

In-source dissociation of peptides crosslinked with SuDP

For our CID-CXL-MS/MS reagents to be effective, the selective dissociation of an intact crosslinked complex within the linker region of the reagent needs to produce both intact individual peptides with significant intensity while simultaneously minimizing peptide backbone fragmentation. Figure 3 demonstrates the effectiveness of the ISCID dissociation approach with two sets of crosslinked peptides, [M1-R8]∼[K9-R15] (abbreviated as M_1∼M_2) and [M1-R8] ∼[D32-K47] (abbreviated as M_3∼M_4). When no additional ISCID energy is applied, the +2, +3, and +4 charge states of the M_1∼M_2 intact crosslinked complex are the most abundant ions (Fig. 3(A)). The individual peptide products are also detectable in this spectrum, a result of the lability of the aspartyl-prolyl bond within the SuDP reagent. In the subsequent CID-CXL dissociation scan (Fig. 3(B)), the application of 15 V of potential offset results in the dissociation of the M_1∼M_2 crosslinked complex with an increase in the relative abundance of the $[M_2P+2H]^{2+}$ and $[M_1SuD+2H]^{2+}$ peptide ions from 7 and 15% to 73 and 74%, respectively. While both individual peptides significantly increased in relative ion abundance, they are only moderately more abundant than the +3 charge state of the intact complex and are still less abundant than the +2 intact crosslinked complex. For a lower abundant crosslink, M_3∼M_4, the ISCID dissociation was less effective. In the survey MS scan, the +2, +3, and +4 charge states of the intact crosslinked complexes are observed along with each sodium adduct containing two Na^+ ions per charge state (Fig. 3(C)). Dissociation of the crosslinked complexes by addition of 15 V of potential offset produces a more complicated spectrum with the only detectable individual peptide ion being $[M_3P+2H]^{2+}$ (Fig. 3(D)). The data-dependent selection of ions using ISCID-MS^2 would preclude MS/MS analysis, and hence identification, of both individual peptide ions generated from the crosslinked complex.

Based on the number of crosslinks identified for AbrBN, 15 V of potential offset works reasonably well for dissociating most crosslinked peptides, but there are exceptions. The decreased efficiency of crosslinked complex dissociation into individual peptides could be a function of peptide length, lysyl residue position within the peptide, or the abundance of the crosslinked complex during ESI. When the dissociation of the crosslinked complex produces ions with sufficient intensity to promote data-dependent MS/MS, the selection of the individual peptides is still being made from a scan event in which any other non-crosslinked peptides eluting at the same time could be selected as well, thus lowering the probability of selecting the ions of interest. Although the ISCID-MS^2 approach could be modified to include selected-ion monitoring to conduct MS/MS on both peptides

DOI: 10.1002/rcm

Table 1. Identified crosslinks of AbrBN using the SuDP reagent and the ISCID-MS^2 acquisition approach

Protein: crosslinker ratio	Protease	Peptide[a]	Complex mass calculated[b]	Complex mass measured[c]	Intact complex[d] charge states	Crosslinked residue	Scan number	Charge state	Xcorr[e]	ΔC_n[f]
Interpeptide crosslinks										
1:2	Trypsin	[9]K#VDELGR[15]	2017.1	2016.6	+2, +3, +4	K2∼K9	2838	2	2.178	0.249
		[1]M@K*STGIVR[8]					2839	2	2.048	0.341
		[9]K#VDELGR[15]	2001.1	2000.8	+2, +3, +4	K2∼K9	2989	1	1.952[g]	0.369
		[1]MK*STGIVR[8]					2994	2	1.747	0.230
1:5	Trypsin	[1]M@K*STGIVR[8]	2017.1	2017.0	+2, +3, +4	K2∼K9	2829	2	1.334[g]	0.213
		[9]K#VDELGR[15]					2833	2	2.483	0.436
		[9]K#VDELGR[15]	2001.1	2000.9	+2, +3, +4	K2∼K9	2996	2	2.539	0.421
		[1]MK*STGIVR[8]					2997	2	1.445[g]	0.052
Intrapeptide crosslinks										
1:2	Trypsin	[1]MK#STGIVRK*VDELGR[15]	1983.1	1982.9	+2, +3	K2∼K9	4083	2	1.854	0.220
1:2	Chymotrypsin	[1]MK#STGIVRK*VDELGRVVIPIEL[22]	2747.1	2746.6	+2, +3	K2∼K9	4926	2	2.565	0.243
		[1]MK#STGIVRK*VDEL[13]	1768.9	1769.2	+1, +2, +4	K2∼K9	4058	2	1.644	0.139
1:5	Trypsin	[1]MK#STGIVRK*VDELGR[15]	1983.1	1982.7	+2, +3	K2∼K9	4116	2	1.503	0.008
		[32]DALEIYVDDEK*IILK#K[47]	2198.2	2198.1	+2, +3	K42∼K46	4801	2	2.096	0.261
1:5	Chymotrypsin	[27]GIAEK#DALEIYVDDEKIILKK*Y[48]	2859.5	2859.8	+2, +3	K31∼K47	4070	2	2.459	0.247
		[1]MK*STGIVRK#VDELGRVVIPIEL[22]	2747.1	2746.3	+2, +3	K2∼K9	4374	2	2.224	0.105

[a] Mass modifications: #, P (97.1 u); *, SuD (197.1 u); @, oxidation (16.0 u).
[b] Average mass calculated for the neutral peptide crosslinked complex.
[c] Average measured mass for the neutral peptide crosslinked complex following deconvolution of the survey MS spectrum.
[d] Observed charge states of the intact crosslinked peptide complex from the precursor MS spectrum prior to the ISCID dissociation event.
[e] SEQUEST generated cross-correlation score.
[f] Delta cross-correlation values (ΔC_n) provide a measure of confidence between the top two peptides identifed for a given product ion spectrum.
[g] Product ion spectra were manually verified for sufficient ion coverage.

DOI: 10.1002/rcm

RCM

Table 2. Identified crosslinks of AbrBN using the SuDP reagent and the ITCID-MS^3 acquisition approach

Protein:crosslinker ratio	Protease	Product[a] ion spectra	Peptide[b]	Complex mass calculated[c]	Complex mass measured[d]	Observed[e] complex charge states	Crosslinked residue	Scan number	Charge state	Xcorr[f]	ΔC_n[g]	Group[h] Xcorr	Group[i] ΔC_n
Interpeptide crosslinks													
1:2	Trypsin	MS^3	[1]M@K*STGIVR[8]	2017.1	2016.8	+2, +3, +4	K2∼K9	3176	2	1.508	0.069	2.066	0.256
			[9]K#VDELGR[15]					3177	2	1.651	0.254	3.381	0.375
			[9]K#VDELGR[15]	1991.1	1991.5	+2, +3, +4	K9∼K47	3336	2	1.855	0.277	3.381	0.375
			[47]K*YKPNMT[53]					3337	2	1.353	0.355	1.384	0.353
			[9]K#VDELGR[15]	2001.1	2000.9	+2, +3, +4	K2∼K9	3476	2	2.400	0.333	3.733	0.443
			[1]MK*STGIVR[8]					3477	2	1.586	0.206	1.442	0.094
1:5	Trypsin	MS^3	[9]K*VDELGR[15]	2001.1	2000.7	+2, +3, +4	K2∼K9	2515	1	1.397	0.213	1.344	0.173
			[1]MK#STGIVR[8]					2516	1	1.601	0.330	1.852	0.145
			[1]M@K*STGIVR[8]	2017.1	2016.8	+2, +3, +4	K2∼K9	3320	2	0.863	0.135	1.446	0.014
			[9]K#VDELGR[15]					3321	2	1.518	0.361	3.199	0.418
			[9]K#VDELGR[15]	2001.1	2000.7	+2, +3, +4	K2∼K9	3464	2	2.224	0.343	3.507	0.340
			[1]MK*STGIVR[8]					3465	2	1.261	0.059	1.479	0.143
			[32]DALEIYVDDEK*IILKK[47]	3090.4	3090.0	+2, +3, +4, +5	K2∼K42	4884	2	1.023	0.016	1.338	0.012
			[1]MK#STGIVR[8]					4885	2	1.283	0.038	1.283	0.038
Intrapeptide crosslinks													
1:2	Chymotrypsin	MS^2	[46]K*KYK#PNMT[53]	1303.3	1303.3	+2, +3	K46∼K49	1551	2	2.157	0.206		
			[38]VDDEK#IILK*KY[48]	1657.7	1656.7	+2, +3	K42∼K46	4355	2	1.461	0.140		
			[1]MK#STGIVRK*VDELGRVVIPIEL[22]	2747.1	2746.3	+2, +3, +4	K2∼K9	5251	2	2.621	0.164		
			[1]MK*STGIVRK#VDELGRVVIPIEL[22]	2747.1	2746.0	+2, +3, +4	K2∼K9	5415	2	3.096	0.075		
1:5	Trypsin	MS^2	[43]IILK*K#YKPNMT[53]	1642.8	1643.3	+1, +2, +3	K46∼K47	3370	2	2.087	0.060		
			[1]MK#STGIVRK*VDELGR[15]	1983.1	1982.0	+2	K2∼K9	3610	2	2.156	0.132		
			[1]MK#STGIVRK*VDELGRVVIPIELRR[24]	3059.5	3058.9	+2, +3	K2∼K9	4314	3	3.641	0.035		
			[32]DALEIYVDDEK*IILK#K[47]	2199.3	2199.5	+2, +3	K42∼K46	5351	2	1.716	0.001		
1:5	Chymotrypsin	MS^2	[1]MK*STGIVRK#VDELGRVVIPIEL[22]	2747.1	2746.4	+2, +3	K2∼K9	4456	2	2.311	0.148		
			[1]MK#STGIVRK*VDELGRVVIPIEL[22]	2747.1	2746.4	+2, +3	K2∼K9	4492	2	2.863	0.108		

[a] The type of product ion spectrum used to identify the peptide.
[b] Mass modifications: #, P (97.1 u); *, SuD (197.1 u); @, oxidation (16.0 u).
[c] Average mass calculated for the neutral peptide crosslinked complex.
[d] Average measured mass for the neutral peptide crosslinked complex following deconvolution of the survey MS spectrum.
[e] Observed charge states of the intact crosslinked peptide complex from the precursor MS spectrum prior to the MS^2 dissociation event.
[f] SEQUEST generated cross-correlation score.
[g] Delta cross-correlation values (ΔC_n) provide a measure of confidence between the top two peptides identifed for a given product ion spectrum.
[h] SEQUEST generated cross-correlation score with integration of all product ion spectra for a precursor ion with the same m/z ratio within a 30 s elution window.
[i] Delta cross-correlation values (ΔC_n) with integration of all product ion spectra for a precursor ion with the same m/z ratio within a 30 s elution window.

DOI: 10.1002/rcm

RCM

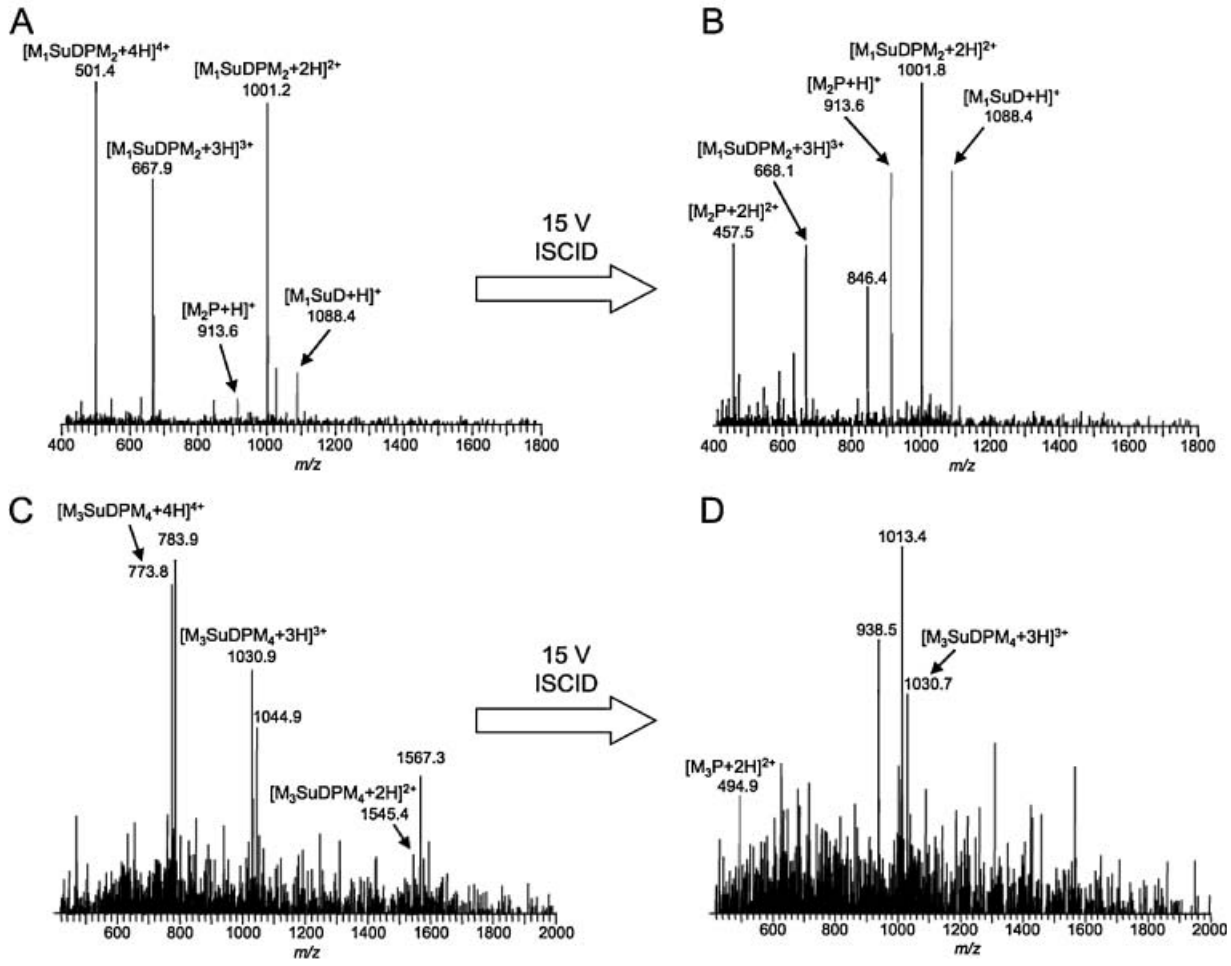

Figure 3. ISCID of two crosslinked peptide complexes from AbrBN. (A) A survey MS spectrum containing the [M1-R8]∼[K9-R15] (M_1∼M_2) crosslinked complex with readily detectable ions of the +2, +3 and +4 charge states at *m/z* 1001.2, 667.9, and 501.4, respectively. (B) Following ISCID using 15 V, individual peptides originating from the intact crosslinked complex are produced: $[M_1SuD+H]^+$ and $[M_2P+H]^+$at *m/z* 1088.4 and 913.6, respectively. The +2, +3 and +4 charge states of the intact crosslinked complex are also present. (C) A survey MS spectrum containing the [M1-R8]∼[D32-K47] (M_3∼M_4) crosslinked complex with ions of the +2, +3, and +4 charge states at *m/z* 1545.4, 1030.9, and 773.8, respectively. Also present are the ions corresponding to sodium adducts of the crosslinked complex. (D) Following ISCID using 15 V, the $[M_3P+2H]^{2+}$ ion at *m/z* 494.9 is the only detectable peptide derived from the M_3∼M_4 crosslinked complex.

generated from the CID-CXL complex, knowledge of the peptide-peptide crosslink mass and the resulting P- and SuD-modified peptides is required.

In-trap dissociation of peptides crosslinked with SuDP

To assess if the additional crosslinks identified in the ITCID-MS^3 approach were due to a more efficient dissociation event than with the ISCID-MS^2 approach, the same set of peptide-peptide crosslinks, M_1∼M_2 and M_3∼M_4, were examined. In the survey MS scan of M_1∼M_2 (Fig. 4(A)), the +2, +3, and +4 charge states of the complex are the most abundant with the signal-to-noise ratios and intensities similar to the survey MS scan in the ISCID-MS^2 approach (Fig. 3(A)). In the subsequent CID-CXL dissociation scan, the +2 intact crosslinked complex (*m/z* of 1001.7) was data-dependently selected and subjected to in-trap CID with a normalized collision energy of 45% (Fig. 4(B)). The crosslinked complex is preferentially cleaved at the aspartyl-prolyl bond within the crosslinking reagent to produce the P- and SuD-modified peptides with barely detectable fragmentation of either peptide backbone. Overall, the relative abundance of $[M_2P+H]^+$ and $[M_1SuD+H]^+$ ions increases from 12 and 7% to 98 and 100% using ITCID.

This reduction in spectral complexity for CID-CXL dissociation within the ion trap had a dramatic effect for the lower abundant M_3∼M_4 crosslinked complex. The survey MS scan for the M_3∼M_4 peptide-peptide crosslink is shown in Fig. 4(C). For this crosslink, the +2, +3 and +4 charge states of the intact crosslinked complex are the most abundant and is similar to the spectrum generated in the ISCID-MS^2 approach (Fig. 3(C)). During the subsequent CID-CXL dissociation scan, the +4 intact crosslinked complex (*m/z* of 773.6) was data-dependently selected and subjected to

DOI: 10.1002/rcm

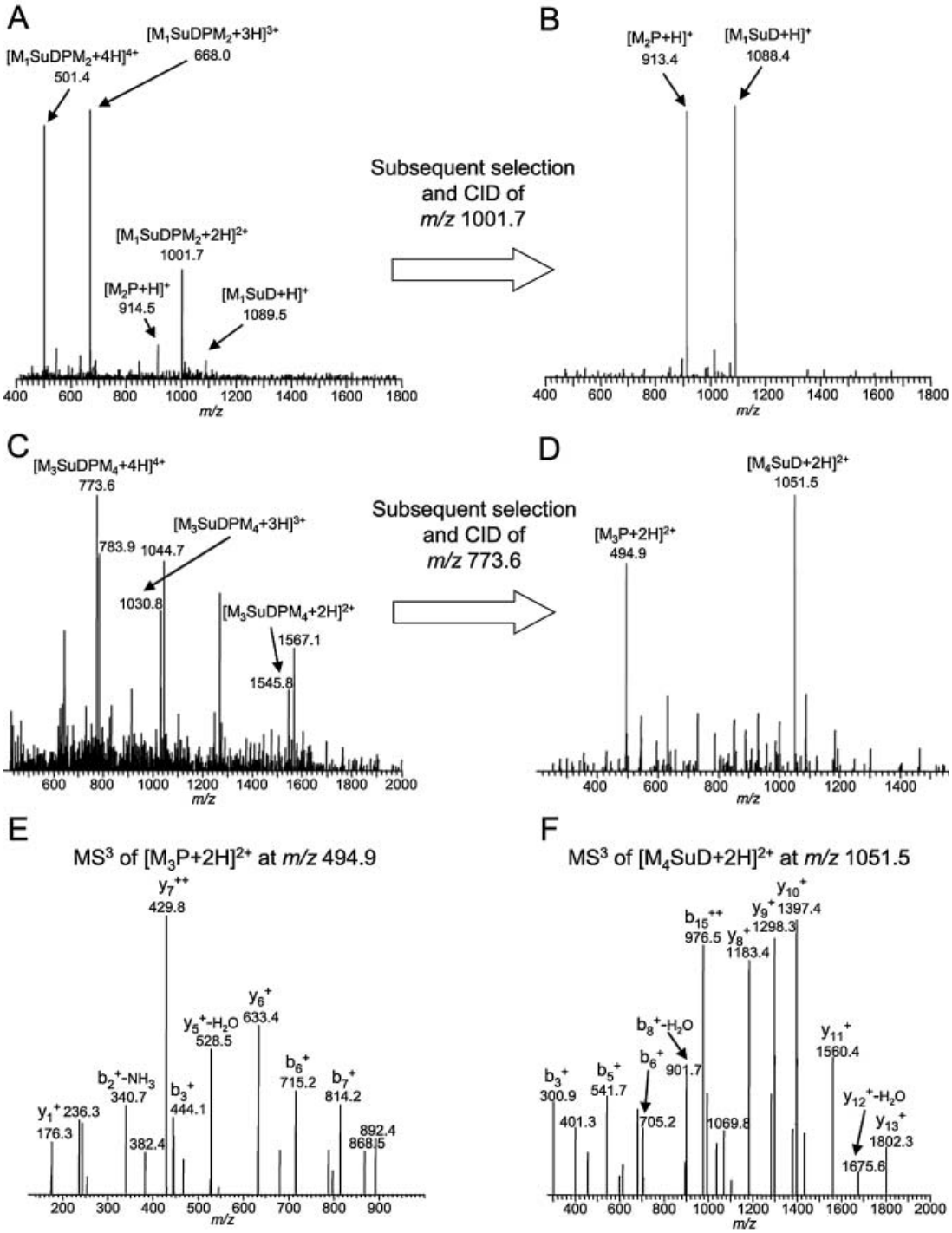

Figure 4. ITCID of two crosslinked peptide complexes from AbrBN. (A) A survey MS spectrum of the [M1-R8]∼[K9-R15] (M_1∼M_2) crosslinked complex with readily detectable ions of the +2, +3, and +4 charge states at *m/z* 1001.7, 668.0, and 501.4, respectively. (B) Following subsequent capture and MS^2 of the ions at *m/z* 1001.7, individual peptides originating from the intact crosslinked complex are produced: $[M_1SuD+H]^+$ and $[M_2P+H]^+$ at *m/z* 1088.4 and 913.4, respectively. (C) A survey MS spectrum containing the [M1-R8]∼[D32-K47] (M_3∼M_4) crosslinked complex with ions of the +2, +3, and +4 charge states at *m/z* 1545.8, 1030.8, and 773.6, respectively. Also present are the ions corresponding to sodium adducts of the crosslinked complex. (D) Following subsequent capture and MS^2 of the ions at *m/z* 773.6, individual peptides originating from the intact crosslinked complex are produced: $[M_3P+2H]^{2+}$ and $[M_4SuD+2H]^{2+}$ at *m/z* 494.9 and 1051.5, respectively. In contrast to Figs. 3(B) and 3(D), the peptide product ions have a significantly higher relative abundance through selective in-trap dissociation of each crosslinked complex. This is important for successful implementation of automated data-dependent acquisitions where the peptide ions of $[M_3P+2H]^{2+}$ and $[M_4SuD+2H]^{2+}$ in (D) are selected for further CID based on their intensity to generate product ion spectra (E) and (F), respectively. These spectra contain a significant number of b and y ions with sufficient intensity which can be interpreted using database searching.

DOI: 10.1002/rcm

in-trap CID using a normalized collision energy of 45% (Fig. 4(D)). The two most abundant ions, $[M_3P+2H]^{2+}$ at *m/z* 494.9 and $[M_4SuD+2H]^{2+}$ at *m/z* 1051.5, are derived from the intact complex and the spectrum presents a marked improvement over the spectrum produced by the ISCID approach in Fig. 3(D). Consequently, data-dependent selection of the $[M_3P+2H]^{2+}$ and $[M_4SuD+2H]^{2+}$ ions is easily achieved to allow further fragmentation to generate product ions (Figs. 4(E) and 4(F)) that enable identification by database searching using SEQUEST (Table 2).

Database searching of product ion spectra

On the basis of each data acquisition scheme, the identification of each peptide for a given crosslink using data generated by ISCID-MS^2 or ITCID-MS^3 was slightly different. To recognize crosslinked peptides via charge-dependent Xcorr values for ISCID-MS^2, the survey MS spectrum was inspected for the presence of the intact crosslinked complex at the calculated *m/z*. In addition, features of the CID-CXL dissociation spectrum can be used to distinguish intermolecular and intramolecular crosslinks. For intermolecular crosslinks, the presence of both individual peptides generated by fragmentation at the aspartyl-prolyl bond within the crosslinking reagent is observed. For intrapeptide crosslinked peptides, the fragmentation of the aspartyl-prolyl bond during the dissociation event does not result in a net change in *m/z* (fragmentation mechanism of Fig. 1(B)), thus an ion with the same *m/z* is observed in both the survey MS spectrum and the CID-CXL dissociation spectrum.

For ITCID-MS^3, dissociation of the crosslinked complex at the MS^2 event produces the two modified peptides that are subsequently fragmented at the MS^3 event. However, the charge-state-dependent Xcorr values were lower for the MS^3 spectra than those for the product ion spectra generated by ISCID-MS^2 due to lower ion abundance and coverage resulting from the additional stage of MS isolation and fragmentation. This phenomenon was also observed using an MS^2-MS^3 approach for phosphopeptide analysis in which ions produced by a neutral loss of phosphoric acid (49.0 or 98.0 u) during an MS^2 scan were data-dependently selected for additional fragmentation with MS^3 analysis.[22] Consequently, charge-dependent Xcorr thresholds were initially lowered due to the decreased efficiency of MS^3 peptide fragmentation. Since lowering these thresholds increases the frequency of misidentification, the presence of the intact crosslinked complex at the calculated *m/z* in the survey MS spectrum and the presence of both modified peptides in the subsequent CID-CXL dissociation spectrum (MS^2 spectrum) were required for each crosslink identification. For crosslinked peptide complexes that met these additional identification criteria, the MS^3 product ion spectra were then re-searched with SEQUEST using group scanning. This feature integrates all product ion spectra originating from the same precursor ion within a 30 s window (i.e, during peak elution) to generate a single integrated spectrum for database matching. For both the MS^2 and MS^3 events, spectral grouping resulted in slightly higher SEQUEST scores for peptides than obtained when only using individual product ion spectra. For the MS^2 data obtained using ISCID, integrated and individual product ion spectra elicited nearly identical SEQUEST scores.

Efficiency of in-source and in-trap crosslinked complex dissociation

To further assess the efficiency of crosslinked peptide complex dissociation from ISCID and ITCID, the ion intensities of the individual peptides from the $M_1{\sim}M_2$ crosslinked complex were plotted as a percentage of the total ion current (TIC) during peak elution (Fig. 5). Using 15 V of potential offset during ISCID, each singly charged peptide contributes to only a maximum of 10% of the TIC. Because additional ISCID energy tends to promote the lower charge states due to proton losses (illustrated in Fig. 3), the intensity of the doubly charged ions corresponding to the same peptides was considerably lower contributing a maximum of 5% of the TIC during peak elution (Fig. 5(A)). At maximum peak

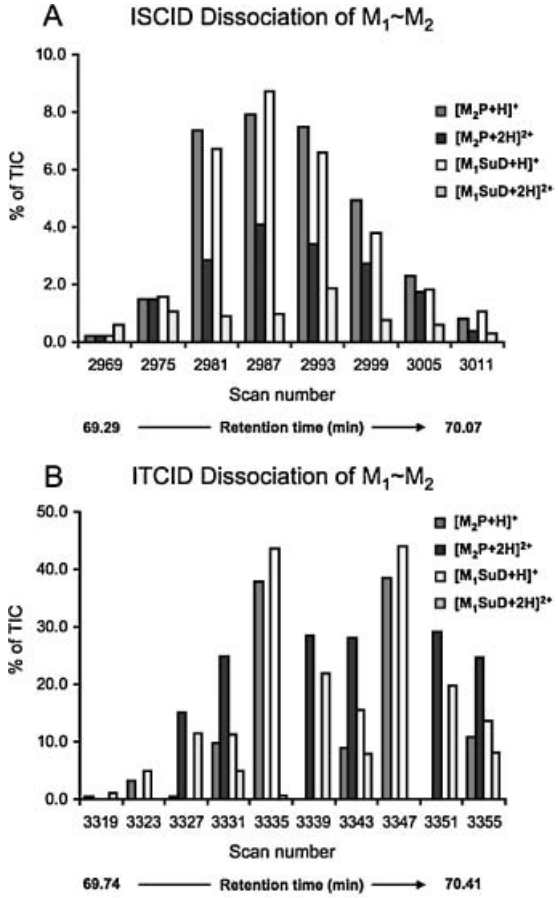

Figure 5. ISCID and ITCID dissociation efficiency of the [M1-R8]∼[K9-R15] ($M_1{\sim}M_2$) crosslinked peptide complex from AbrBN. The relative intensity of the M_1SuD and M_2P peptide product ions obtained using (A) ISCID or (B) ITCID are plotted according to their percentage of the total ion current (TIC) during elution of the $M_1{\sim}M_2$ peptide-peptide crosslink. For ISCID, the efficiency of dissociation leading to the emergence of the individual peptides for all charge states is relatively low, eliciting a maximum contribution of 22% to the TIC at scan 2987. For ITCID, the efficiency of crosslinked complex dissociation within the ion trap is significantly higher when compared to ISCID, eliciting a maximum contribution of 82% to the TIC at scan 3335.

DOI: 10.1002/rcm

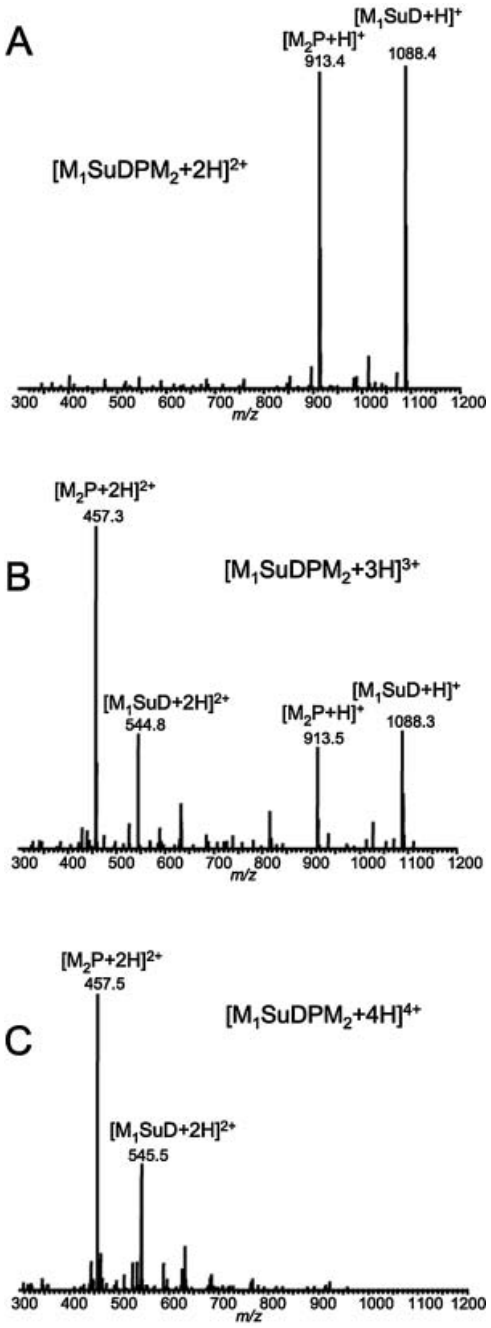

Figure 6. MS^2 spectra for the in-trap CID-CXL dissociation of the [M1-R8]∼[K9-R15] (M_1∼M_2) crosslinked complex from AbrBN. Based on the (A) +2, (B) +3, and (C) +4 charge state of the M_1∼M_2 complex, ions corresponding to products M_1SuD and M_2P are generated. These products vary according to intensity and charge state based on the CID channels for the given charge state of the intact M_1∼M_2 complex and presumably to the amino acid sequence of each peptide and the site of the modification. In all MS^2 spectra, at least one charge state from both peptides is produced with sufficient intensity to elicit data-dependent selection and subsequent fragmentation during the MS^3 event to generate spectra that can be analyzed using database searching.

intensity (scan 2987), the sum of all of the individual peptides obtained using ISCID contributed to 22% of the TIC. This indicates that 78% of the TIC is composed of the residual intact crosslinked peptide complex which was not dissociated, ions of co-eluting peptides, non-specific ion fragmentation, and background noise. When the same M_1∼M_2 crosslinked complex was analyzed by the ITCID-MS^3 approach, significant improvements were readily apparent. First, the contribution of the intact individual peptides to the TIC was significantly higher using ITCID. For scan 3335, the sum of all of the intact individual peptides contributing to the TIC was 82%, a significant increase from the 22% for the same crosslinked peptide complex when dissociated using ISCID. Second, every scan contained an ion of sufficient intensity for each M_1SuD and M_2P peptide although the charge stated varied. This is important because both of the peptides from each crosslinked complex must be subsequently selected and fragmented for identification.

To determine if the varying charge states for the individual peptides was mediated by the charge state of the intact

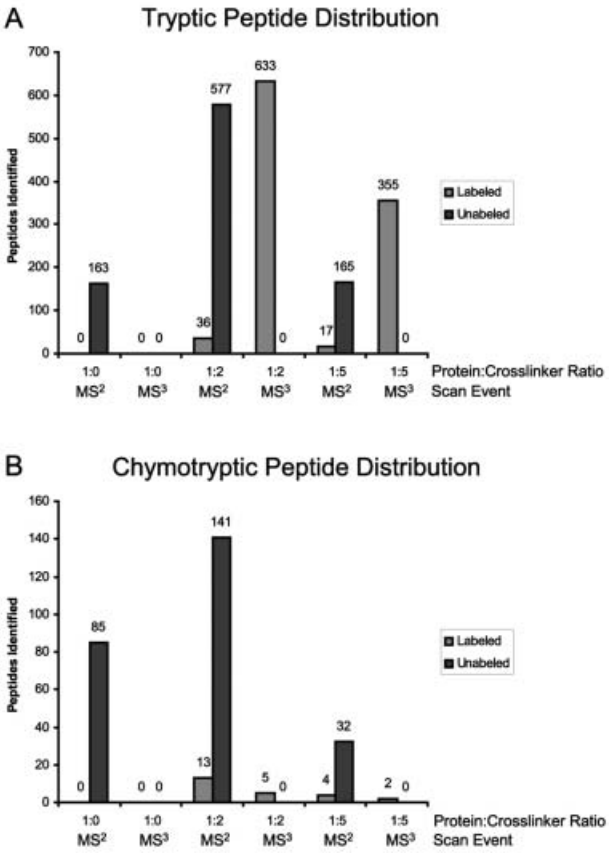

Figure 7. Peptide distribution of AbrBN peptides identified using the ITCID-MS^3 approach and database searching. For crosslinked AbrBN digested with (A) trypsin or (B) chymotrypsin, the number of recognized labeled and unlabeled peptides is plotted according to their identification using the product ion spectra generated by the MS^2 or MS^3 event. Considering all the labeled peptides identified in the trypsin and chymotrypsin treated samples, 95% and 29% were obtained from the MS^3 spectra. This difference was due to the distribution of unique intra- and interpeptide crosslinks present in each sample after proteolytic digestion. Based on the gas-phase chemistry of the aspartyl-prolyl bond within the crosslinker, interpeptide crosslinks and dead-end products were identified in the MS^3 spectra and intrapeptide crosslinks and unlabeled peptides were identified using the MS^2 spectra.

DOI: 10.1002/rcm

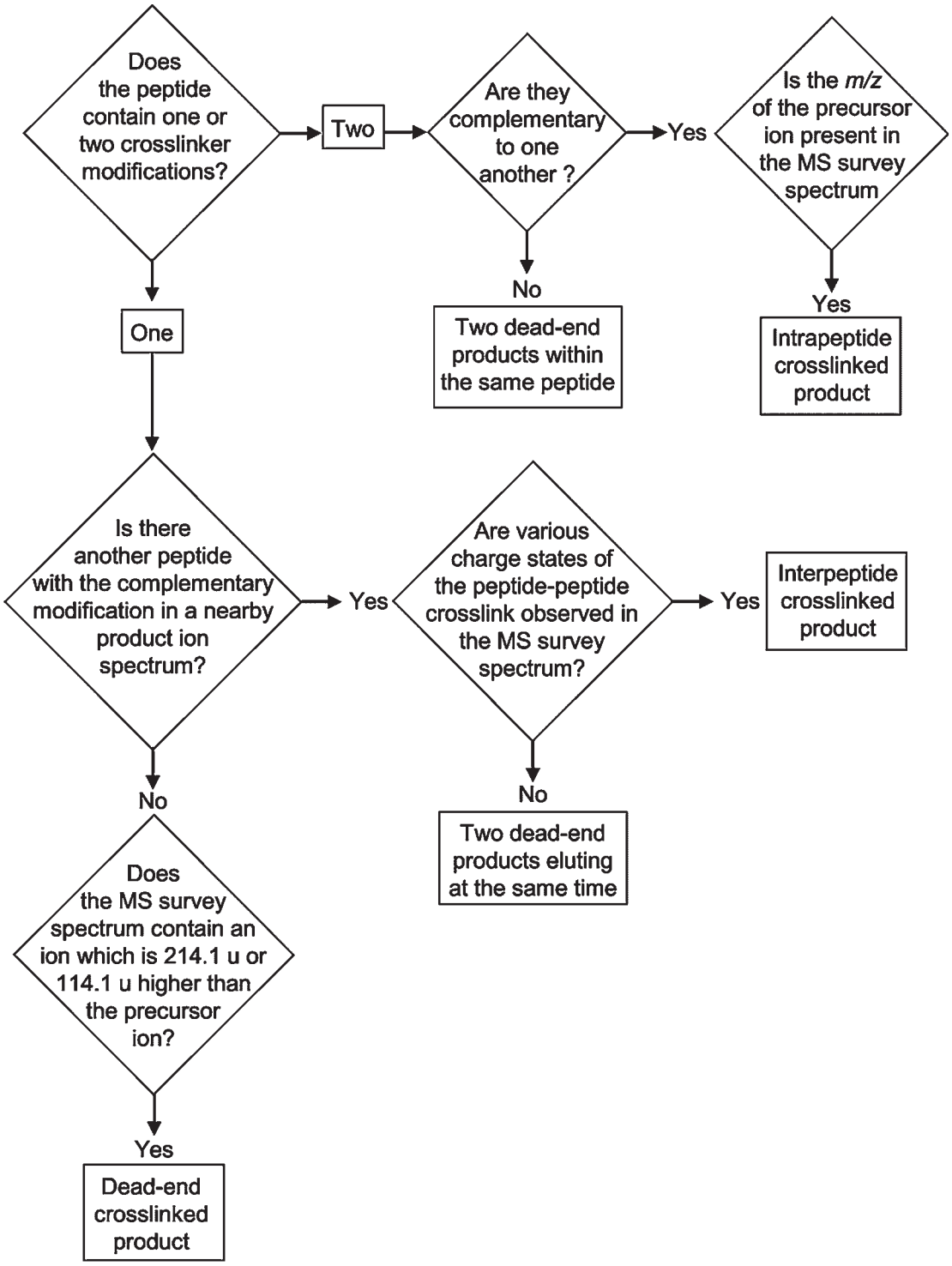

Figure 8. Decision tree for the identification of interpeptide, intrapeptide, and dead-end crosslinks using CID-CXL-MS/MS reagents and the ITCID-MS^3 acquisition approach. All peptides identified by SEQUEST as containing crosslinker modifications of either an SuD (197.1 u), a P (97.0 u), or both (SuD and P) on lysyl residues can be further processed (starting at the upper left) to ascertain the nature of the crosslink. Complementary modifications refer to the condition where an SuD-modification on one lysyl residue or peptide can be paired to a P-modification on another lysyl residue on the same peptide or another peptide, and vice versa. Mass modifications of 214.1 or 114.1 u correspond to crosslinker-derived fragments in the free acid form, SuD-OH for peptides containing P-modifications and P-OH for peptides containing SuD-modifications, respectively, which are generated from the presence of a dead-end crosslinked product.

DOI: 10.1002/rcm

crosslinked complex, spectra obtained for the in-trap CID-CXL scan event for the +2, +3, and +4 charge states of the $M_1{\sim}M_2$ crosslinked complex were examined (Fig. 6). Dissociation of the +2 complex produces both P- and SuD-modified peptides each having a +1 charge state, presumably due to each peptide containing a C-terminal arginyl residue that has a high affinity for a mobile proton from the intact complex. Upon dissociation of the +3 complex, both the +1 and +2 charge states of the individual peptides are observed, with the third proton having a preference for the M_2P peptide relative to the M_1SuD peptide in a 2.5:1 abundance ratio. For the +4 complex, both peptides each have two protons, but there is a similar preference for the M_2P peptide as observed for the products of dissociation of the +3 complex. When considering all charge states of the M_2P and M_1SuD products generated in-trap by fragmentation of the intact crosslinked complexes, the efficiency of CID-CXL dissociation is 82, 62 and 53% for the +2, +3, and +4 charge states, respectively. The reduced efficiency for higher order charge states containing more than two protons can be explained by the increase in peptide backbone fragmentation. Although additional backbone fragmentation is observed, both P- and SuD-modified peptides are by far the most abundant ions and thus would be data-dependently selected for additional fragmentation using our automated approach. In addition, MS^3 analysis of various charge states of an individual peptide will benefit identification because different charge states will result in different product ion spectra for database searching.

Considering that the normalized collision energy setting of 45% for the LCQ Deca ion trap is used to achieve complete fragmentation of peptides, the aspartyl-prolyl bond within our crosslinker provides a dissociation channel that appears to minimize simultaneous amide bond cleavage within both peptides. Although more work using synthetically designed peptides, including a peptide containing an aspartyl-prolyl bond, is necessary to further characterize the CID-CXL dissociation event, our initial crosslinker design seems to be well suited for CID using ion traps. Unfortunately, because of the nature of data-dependent selection and MS^n experiments permitted by the LCQ Deca ion trap, we were not able to perform the MS^2 event at a lower normalized collision energy setting and the MS^3 event at a higher energy setting, thus the use of ISCID-MS^2 could be advantageous. Other instrument configurations such as a triple quadrupole-linear ion trap mass spectrometer could be implemented in which the low-energy CID event could be performed using the collisional quadrupole and the generated P- and SuD-modified peptides subsequently fragmented at higher-energy CID in the ion trap.

Distribution of the crosslinked products of AbrBN

When the AbrBN samples were analyzed using the ITCID-MS^3 acquisition approach, interpretable product ion spectra were produced by both the MS^2 and MS^3 events. Since the peptides present in each sample are either labeled with the crosslinking reagent or remain unlabeled, the distribution of the total number of identified labeled and unlabeled peptides from both sets of data were plotted according to the various protein-to-crosslinker ratios and treatment with either trypsin (Fig. 7(A)) or chymotrypsin (Fig. 7(B)). For this analysis, all peptides which contained either the P- or SuD-modification at a lysyl residue during either CID event were included. The number of individually P-or SuD-labeled peptides is significantly higher than the number of crosslinks identified because these identifications include peptides involved in dead-end crosslinked products in which one end of the crosslinking reagent was hydrolyzed to generate a carboxylic acid functionality and intrapeptide crosslinks in which each modification is present on two lysyl residues within the same peptide.

The data presented in Fig. 7 revealed that all of the unlabeled peptides were identified in the MS^2 spectra. This is consistent with the applied normalized collision energy setting of 45% that is sufficient to elicit peptide amide bond cleavage. However, 5% and 29% of the MS^2 spectra for samples treated with trypsin and chymotrypsin, respectively, were determined to have been generated by a peptide containing both a P- and SuD-modification. Manual inspection of the product ions based on the corresponding precursor ion mass indicated that these labeled peptides each contained an intrapeptide crosslink where the limited rotational freedom about the aspartyl-prolyl bond of the crosslinker produces a dissociation channel equivalent to the amide bonds of the peptide backbone, thus generating detectable b and y ions. For the MS^3 spectra, a higher percentage of labeled peptides were identified corresponding to 95% and 29% for samples treated with trypsin and chymotrypsin, respectively, and contained either a P- or SuD- modification. Inspection of the preceding MS^2 spectrum and its corresponding precursor ion mass revealed that the labeled peptides recognized in the MS^3 spectra were generated from either an interpeptide crosslink or dead-end product. Thus the CID energy used during the MS^2 event for these derivatives is primarily channeled to the aspartyl-prolyl bond fragmentation pathway to facilitate dissociation of the crosslinked complex, not peptide amide bond backbone fragmentation as observed for the intrapeptide crosslinks. Overall, the use of the ITCID-MS^3 acquisition approach with our CID-CXL-MS/MS reagents permits the segregation of intrapeptide and interpeptide crosslinks exclusively into MS^2 and MS^3 spectra, respectively, and when combined with the corresponding precursor ion mass, provides a mechanism for constructing an automated method to identify peptide crosslinks (Fig. 8).

CONCLUSIONS

A comparison between ISCID and ITCID for selective low-energy dissociation for several different crosslinked peptides from AbrBN using our SuDP CID-CXL-MS/MS reagent revealed that performing this event within the ion trap results in several analytical advantages regarding crosslink identification. First, the CID-CXL spectra (the MS^2 event) were less complicated due to ions being generated from a single crosslinked complex. This proved to be essential for subsequent CID analysis because it increased the likelihood that both individual peptides would be the most abundant

DOI: 10.1002/rcm

ions and thus selected during the data-dependent acquisition. Second, the amount of applied CID energy that is typically used to fragment peptide backbone amide bonds is primarily channeled to the aspartyl-prolyl bond of the crosslinking reagent. Although other dissociation channels become available at higher charge states, the major ions are those of the distinct P- or SuD-modified peptide products. Third, the ITCID-MS^3 approach results in two separate sets of product ion spectra which can be subjected to database searching. Based on the gas-phase ion chemistry of the aspartyl-prolyl bond, only peptides as part of interpeptide crosslinks and dead-end products were identified in the MS^3 spectra and intrapeptide crosslinks were identified in the MS^2 spectra, which lends itself to more automated data analysis. Overall, our CID-CXL-MS/MS technology represents a novel way to rapidly evaluate critical protein-protein interactions by tandem mass spectrometry. Based on this study, it can be used to elucidate multimer orientation and domain organization in proteins which will aid in the assignments of distance constraints used in NMR structure determination. To further refine our approach, the use of other MS platforms or reagents containing alternative CID-CXL functionalities such as other amino acid substitutions (Xxx-Pro) to the Asp- Pro bond or mono-oxidized thioethers are being investigated.[23,24] This may provide a high-throughput alternative to evaluate targets within pharmaceutical discovery programs that involve the study of intermolecular or intramolecular protein interactions and provide higher order interaction information by TAP-tagging approaches to help identify novel interacting partners to elucidate signal transduction mechanisms.

Acknowledgements

We would like to thank the research agencies of North Carolina State University and the North Carolina Agricultural Research Service for continued support of our biological mass spectrometry research. Portions of this work conducted by E.J.S. and M.B.G. were supported by grants from the National Science Foundation (MCB-0419819) and the United States Department of Agriculture (NRI 2004-35304-14930 and NRI 2005-35604-15420). Portions of this work conducted by B.G.B. and J.C. were supported by NIH GM55769. We also thank Kevin Blackburn for critical reading of the manuscript.

REFERENCES

1. Sinz A. *J. Mass Spectrom.* 2003; **38**: 1225.
2. van Dijk AD, Boelens R, Bonvin AM. *FEBS J.* 2005; **272**: 293.
3. Taverner T, Hall NE, O'Hair RA, Simpson RJ. *J. Biol. Chem.* 2002; **277**: 46487.
4. Young MM, Tang N, Hempel JC, Oshiro CM, Taylor EW, Kuntz ID, Gibson BW, Dollinger G. *Proc. Natl. Acad. Sci. USA* 2000; **97**: 5802.
5. Sinz A. *Mass Spectrom. Rev.* 2006; **25**: 663.
6. Schilling B, Row RH, Gibson BW, Guo X, Young MM. *J. Am. Soc. Mass Spectrom.* 2003; **14**: 834.
7. Wefing S, Schnaible V, Hoffmann D. *Anal. Chem.* 2006; **78**: 1235.
8. Petrotchenko EV, Olkhovik VK, Borchers CH. *Mol. Cell. Proteomics* 2005; **4**: 1167.
9. Schmidt A, Kalkhof S, Ihling C, Cooper DM, Sinz A. *Eur. J. Mass Spectrom.* 2005; **11**: 525.
10. Hurst GB, Lankford TK, Kennel SJ. *J. Am. Soc. Mass Spectrom.* 2004; **15**: 832.
11. Sinz A, Kalkhof S, Ihling C. *J. Am. Soc. Mass Spectrom.* 2005; **16**: 1921.
12. Back JW, Hartog AF, Dekker HL, Muijsers AO, de Koning LJ, de Jong L. *J. Am. Soc. Mass Spectrom.* 2001; **12**: 222.
13. Tang X, Munske GR, Siems WF, Bruce JE. *Anal. Chem.* 2005; **77**: 311.
14. Green NS, Reisler E, Houk KN. *Protein Sci.* 2001; **10**: 1293.
15. Peters K, Richards FM. *Annu. Rev. Biochem.* 1977; **46**: 523.
16. Soderblom EJ, Goshe MB. *Anal. Chem.* 2006; **78**: 8059.
17. Bobay BG, Andreeva A, Mueller GA, Cavanagh J, Murzin AG. *FEBS Lett.* 2005; **579**: 5669.
18. Coles M, Djuranovic S, Soding J, Frickey T, Koretke K, Truffault V, Martin J, Lupas AN. *Structure* 2005; **13**: 919.
19. Benson LM, Vaughn JL, Strauch MA, Bobay BG, Thompson R, Naylor S, Cavanagh J. *Anal. Biochem.* 2002; **306**: 222.
20. Kluger R, Alagic A. *Bioorg. Chem.* 2004; **32**: 451.
21. Back JW, de Jong L, Muijsers AO, de Koster CG. *J. Mol. Biol.* 2003; **331**: 303.
22. Beausoleil SA, Jedrychowski M, Schwartz D, Elias JE, Villen J, Li J, Cohn MA, Cantley LC, Gygi SP. *Proc. Natl. Acad. Sci. USA* 2004; **101**: 12130.
23. Lagerwerf FM, van de Weert M, Heerma W, Haverkamp J. *Rapid Commun. Mass Spectrom.* 1996; **10**: 1905.
24. Chowdhury SM, Munske GR, Ronald RC, Bruce JE. *J. Am. Soc. Mass Spectrom.* 2007; **18**: 493.

DOI: 10.1002/rcm